HTML ABSTRACT + LINKS

Periodic finite element/boundary element modeling of capacitive micromachined ultrasonic transducers

S. Ballandras, M. Wilm, W. Daniau, A. Reinhardt, V. Laude, and R. Armati
Institut FEMTO-ST, UMR CNRS 6174, Département LPMO, 32 Avenue de l'Observatoire, 25044 Besançon Cedex, France

(Received 13 May 2004; accepted 1 November 2004; published online 30 December 2004)

The possibility to excite and detect acoustic waves in fluids using capacitive transducers built on silicon using surface micromachining offers attractive opportunities in the manufacturing of high quality low cost imaging probes. As in the case of standard probe transducers, simulation codes are required to accurately design such devices. The periodic structures extensively used for these capacitive transducers has to be accounted for. In this work, a two-dimensional finite element analysis of capacitive micromachined ultrasonic transducers (cMUT) is proposed, taking into account periodicity and radiation in fluids. The convergence of the calculation is verified using different computation approaches. It is then shown that the periodic computations provide a rapid and precise analysis of the cMUT compared to non periodic calculations. The mutual displacements are deduced from the periodic harmonic calculation, providing an efficient estimation of cross-talk phenomena arising for cMUT radiating in water. The capability of cMUT operating under such conditions to generate a low velocity wave guided at the fluid/silicon interface is theoretically pointed out. © *2005 American Institute of Physics*. [DOI: 10.1063/1.1839634]

I. INTRODUCTION

The concept of micromachined ultrasound transducer (MUT)[1] gives rise to opportunities in the development of high density integrated imaging devices. The possibility to manufacture ultrasound transducers based on electrostatic forces (as introduced by Khuri-Yakub *et al.*)[1] has received particular interest, from both theoretical and experimental points of view. Many analytical approaches have been proposed to develop efficient tools providing the most important characteristics (coupling, radiation pressure, acoustic impedance, etc.) of simple capacitive muts (cMUTs) architectures (circular shapes of the membrane).[2–4] The simulation of electrostatic excitation and fluid/structure interaction can be accurately performed using most of the commercial finite element analysis (FEA) package (for instance ANSYS).[5] As a consequence, previous work has already been devoted to the numerical simulation of cMUTs by different research groups (e.g., Refs. 1, 5, and 6). However, most of these developments does not rigorously account for the periodicity of the corresponding structures, which is a typical feature of actually implemented cMUTs. The present work proposes a theoretical analysis based on a periodic FEA[7] particularly well suited for providing an accurate, reliable, and fast treatment of such devices.

In the present work, we are investigating the simulation of two-dimensional (2D) capacitive transducers, taking into account the periodicity of the structure and also radiation conditions applied to the device in operation. Inspiring ourselves from the earlier-mentioned work[1,5,6] but also from our own experience in the development of FEA simulation tools devoted to acoustic transducers,[8] and taking advantage of all the work already performed for modelling radiation in fluids (see for instance Ref. 9), we have implemented a computation code allowing us to simulate 2D cMUTs radiating in semi-infinite fluids. It has been performed using a FEA package based on the MODULEF-INRIA toolbox,[10] adapted to the addressed problem. Radiation boundary conditions are taken into account by using a Bloch–Floquet development of the standard Green's function formulation (assuming flat interfaces). The corresponding equations and the results are described in the following sections. This basic development will be used in the future as a basis for a comprehensive three-dimensional model of cMUTs.

Comparisons between simulation results provided by the periodic and nonperiodic computations show the convergence of both approaches for 2D structures. The vanishing of the resonance is clearly proved using the periodic approach for structures excited in phase. However, in almost all the other excitation configuration, one points out the arising of a contribution to the dispersion curve assumed to correspond to a wave traveling along the cMUT array, exhibiting a spectral behavior similar to any wave guided in a periodic structure. The calculation of mutual displacements deduced from the harmonic vibration of the considered cell clearly shows that this wave propagates along the MUT array with a small amount of losses. A simple approach is then proposed to compute the admittance of the cMUT, based on the plane capacitor approximation. This provides an estimation of the actual electrical response of a water-loaded cMUT but it mainly points out the electrical contribution of the earlier mentioned guided wave, as well as the capability of the cMUT to efficiently generate pressure waves in water for different excitation combination.

II. BASIC EQUATIONS AND FEA FORMULATION

A. Simplified model using a uniform excitation

A scheme of the considered cMUT structure is shown in Fig. 1. A Si_3N_4 membrane is assumed stress free, perfectly

 © 2005 American Institute of Physics

Downloaded 21 Jan 2005 to 195.83.19.253. Redistribution subject to AIP license or copyright, see http://jap.aip.org/jap/copyright.jsp

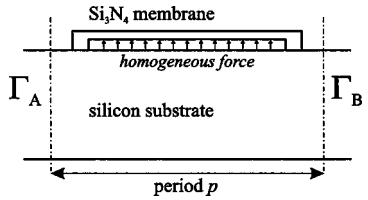

FIG. 1. Scheme of a single cell of a cMUT for the FEA computations. Γ_A and Γ_B are the bounds of the considered period.

flat, and suspended over a silicon wafer (residual stresses are neglected). A homogeneous electrostatic force applied atop the membrane is assumed to actuate the cMUT. The upper side of the membrane can be free of any stress (operation in vacuum) or loaded with a radiation medium (typically water). The cell represented in Fig. 1 consists in an elementary part of an infinite periodic cMUT array.

The basic equations of the problem are those of an elastic problem. A very first step in simulating cMUTs simply consists in considering a uniform force excitation applied on the backside of the cMUT membrane.

The purely elastic FEA formulation is written as follows:

$$\int\int\int_{\Omega}\left(\frac{\partial\,\delta u_i^*}{\partial x_j}C_{ijkl}\frac{\partial u_l}{\partial x_k}-\rho\omega^2 u_i\delta u_i^*\right)dV = \int\int_{\Gamma}\delta u_i^* T_{ij}n_j dS, \tag{1}$$

where u_i is the mechanical displacement, δu_i is the variational unknowns, T_{ij} is the dynamic stress, C_{ijkl} is the elastic constants, ρ is the mass density, and ω is the angular frequency. The classical FEA interpolation procedure is then applied to the mechanical displacement field, yielding the matrix representation of Eq. (2):

$$[K_{uu}-\omega^2 M_{uu}]\{u\}=\{F\}, \tag{2}$$

where K_{uu} and M_{uu} are the stiffness and mass matrices, respectively, and F represents the inner and outer forces exerted on the regarded body. This algebraic system is solved by setting proper boundary conditions, yielding a unique solution of the actual problem. In our case, Neumann conditions corresponding to a uniform force are set to the top side of the membrane (supporting the aluminium electrode) whereas Dirichlet conditions are applied to the backside of the silicon plate (no displacements allowed). Boundary conditions related to the periodic case are discussed in the next paragraph.

In the first computations, no radiation condition is applied and the calculation results from nonperiodic and periodic (fully synchronous) simulations are compared. A period of 50 μm together with an aperture of 40 μm (the "length" of the membrane) are considered, as well as a membrane thickness of 0.5 μm and a gap of 0.5 μm conformably to what is developed experimentally in our project. Numerous sets of data are found in the literature concerning the elastic properties of silicon nitride. We have arbitrary selected one set for which our results are coherent with previously obtained measurements.[11] The mass density of silicon nitride is assumed to equal 3 260 kg/m^3, its elastic constants are as

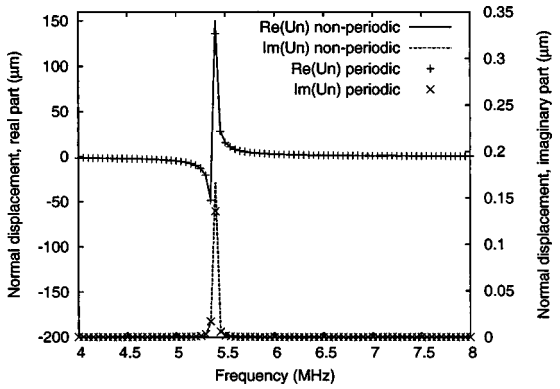

FIG. 2. Comparison between nonperiodic and periodic simulations of an infinite array excited synchronously ($\gamma=0$).

follows $C_{11}=345$ GPa, $C_{12}=125$ GPa, $C_{22}=395$ GPa, $C_{66}=118$ GPa. Silicon elastic properties are those given by Landolt–Börnstein.[4] This yields a resonance frequency in vacuum as found using analytic models and experimentally (more than 5 MHz, cf. Fig. 2).[11] The force was arbitrarily fixed to 4 N, yielding a stress equal to 10^5 Pa (the value actually programmed in the simulation).

B. Simulation of periodic arrays

The same computation is performed using periodic boundary conditions. In that case, the FEA formulation is modified to take into account the dependence of the problem to a so-called propagation coefficient varying from 0 to 1/2, written γ,[7] enabling one to simulate different phase combinations on the boundary of the considered domain. The main benefit of periodic computations consists in reducing the computation to only one period of any periodic array. The latter is then considered infinite in the propagation direction and the use of appropriate boundary conditions is required to accurately take into account the actual operation of the device.

In this approach, the mechanical displacements and the stresses obey a quasiperiodicity law throughout the elementary period, assuming an harmonic force exciting the array[7] as follows:

$$u_i(x_1+np)=u_i(x_1)e^{-j2\pi\gamma n}=u_{i_n}(x_1), \tag{3}$$

$$T_{ij}(x_1+np)=T_{ij}(x_1)e^{-j2\pi\gamma n}=T_{ij_n}(x_1), \tag{3}$$

where x_1 is the spatial coordinate collinear to the periodic array. These relations yield specific boundary conditions at the limits Γ_A and Γ_B of the elementary cell of Fig. 1. These conditions are simply deduced from Eq. (3), and directly relate the degrees of freedom (dof) at boundaries Γ_A and Γ_B:

$$\{u_{\Gamma_B}\}=\{u_{\Gamma_A}\}e^{-j2\pi\gamma}. \tag{4}$$

Note that the spatial distribution of nodes (supporting the dof) on Γ_A and Γ_B must be identical to ensure the coherence of Eq. (3). This relation is then used to simplify the linear algebraic system obtained after interpolation and integration of the Lagrangian expression.[7] Equation (3) imposes that the number of independent variables of the problem is reduced.

Downloaded 21 Jan 2005 to 195.83.19.253. Redistribution subject to AIP license or copyright, see http://jap.aip.org/jap/copyright.jsp

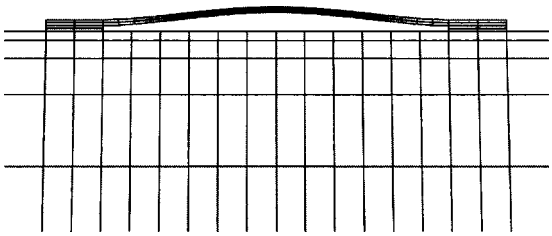

FIG. 3. Vibration shapes of the membrane at 3 MHz.

However, in the present work, the initial number of dof is preserved to avoid matrix reorganizations, considered here as a source of time consumption and yielding too much program complications. In this approach, the following transformation matrix $[T_u]$ is introduced:

$$\begin{Bmatrix} u_{\Gamma_A} \\ u_\Omega \\ u_{\Gamma_B} \end{Bmatrix} = [T_u] \begin{Bmatrix} v_{\Gamma_A} \\ v_\Omega \\ v_{\Gamma_B} \end{Bmatrix} = \begin{bmatrix} I_\Gamma & 0 & 0 \\ 0 & I_\Omega & 0 \\ I_\Gamma e^{-j2\pi\gamma} & 0 & I_\Gamma \end{bmatrix} \begin{Bmatrix} v_{\Gamma_A} \\ v_\Omega \\ v_{\Gamma_B} \end{Bmatrix} \text{ with } \{v_{\Gamma_B}\} = \{0\}, \quad (5)$$

where u_Ω corresponds to the dof of the inner meshed domain (Γ_A and Γ_B excluded), and ν is the new set of dof, taking into account the periodicity condition, used to solve the FEA problem. Equation (5) is then inserted in the standard discrete form of the FEA written as follows for a monochromatic variation of mechanical and electrical fields considered in the problem (time dependence in $e^{j\omega t}$):

$${}^t[T_u^*(\gamma)][K_{uu} - \omega^2 M_{uu}][T_u(\gamma)]\{v\} = {}^t[T_u^*(\gamma)]\{F\}, \quad (6)$$

where upper scripts t and *, respectively, denote a matrix transposition and a complex conjugation. Examples of computations are reported in Figs. 2 and 3. In Fig. 2, periodic and nonperiodic computations are compared. For nonperiodic computations, the displacements along x at boundaries Γ_A and Γ_B are set to zero describing then a symmetric structure at these bounds. In the case of periodic computations, the boundary conditions reported in Sec. II A are used setting the propagation coefficient γ to 0, which corresponds to a synchronous excitation of the array. One can underline the perfect agreement between both results, showing the equivalence of the corresponding boundary conditions. Figure 3 shows the deformed mesh at $\gamma=0$ for a frequency close to the resonance. The fundamental flexural vibration can easily be identified on this result.

C. Radiation of cMUTs in fluids

The analysis of ultrasound transducer operation is generally performed in two steps. The first one consists in the simulation of the device in vacuum, allowing to determine resonance frequencies, coupling coefficients and so on. The second step requires the computation of the transducer radiating in a semi-infinite medium (air or water), assuming a physically acceptable representation of the fluid/structure coupling phenomena. Again in that case, it is desirable to treat both problems of periodic and nonperiodic devices. This enables to take into account any transducer structure, with an accurate treatment of actual operation conditions.

The accurate simulation of radiation conditions in fluids can be obtained by the use of the Green's function approach.[9] The problem of nonperiodic transducer radiating in fluids has been addressed by many authors, see for instance Ref. 12. However, the periodic problem has received a smaller interest. It is then of great importance in the present work to propose an efficient treatment of the periodic problem, well adapted to describe cMUT radiating in water for instance.

In both nonperiodic and periodic cases, radiation conditions are inserted in the right-hand side of Eq. (1), assuming the pressure equilibrium at the fluid/structure interface

$$T_{ij} n_j = -P n_i, \quad (7)$$

where P is the pressure and n_j is the normal to the radiating interface. This latter is then expressed as the convolution between the acoustic contribution of the radiation medium (assumed here semi-infinite) and the displacement normal to the interface, conformably to Green's theory and acoustics laws in fluids.[9] There are mainly two different approaches to derive the Green's function of a semi-infinite fluid in which acoustic waves are radiated (the waves vanish at infinity). The first approach consists in the resolution of the Helmholtz problem in the real space, yielding the pressure as a Hankel function.[13] The second approach consists in solving the problem in the Fourier domain, assuming for instance the propagation of waves in fluids as solution of the corresponding Christoffel equation system.[14] Both approaches lead to equivalent representations of the acoustic behavior of the fluid. The corresponding equations are

$$P(x) = \int_{-\infty}^{+\infty} G(x - x') u_n(x') dx'$$
$$\text{with } G(x - x') = \frac{-j\rho_f \omega^2}{2} H_0^{(2)}(k|x' - x|), \quad (8)$$

where G is the Green's function, H is the Hankel function of second kind and 0th order, s_x is the slowness of the wave along x, k is a wave number equal to ωs_x, and ρ_f is the density of the fluid. Equation (8) is directly inserted in Eq. (1) and the classical FEA interpolation is then applied to the displacements u_n normal to the interface (in most of the treated cases, u_n is arbitrarily taken to be equal to u_2). In the nonperiodic developments, we have considered the expression of the Green's function in the real domain together with a polynomial expansion of the Hankel function allowing for an accurate computation of the fluid contribution. The logarithmic behavior of the Hankel function is explicitly integrated across the polynomial interpolation of the FEA. The resulting system to be solved is still symmetric but exhibits a larger front band due to the connection of all the dof of the radiating area. Nevertheless, no major changes are required in our FEA code to solve the corresponding problem. The contribution of the fluid initially developed in the right-hand side is transferred to the left-hand side of Eq. (1) which is now written as follows

Downloaded 21 Jan 2005 to 195.83.19.253. Redistribution subject to AIP license or copyright, see http://jap.aip.org/jap/copyright.jsp

$$[K - \omega^2 M - X(\omega)]\{u\} = \{F\}, \tag{9}$$

where X represents the frequency dependent radiation matrix.

In the case of periodic problems, the concept of the periodic Green's function G^p[15] must be introduced. The pressure is now also affected by the periodicity of the problem, yielding the following definition of P:

$$T_{ij}n_j = -Pn_i \text{ with } P(x) = \frac{1}{p}\int_{-p/2}^{+p/2} G^p(x-x')u_{\text{normal}}(x')dx'$$
$$\text{and } G^p(x) = \sum_{l=-\infty}^{\infty} \tilde{G}(\gamma + l, \omega)e^{-j\frac{2\pi}{p}(\gamma+l)x}, \tag{10}$$

where p is the period (see Fig. 1). The periodic Green's function is a Floquet expansion of the classical Green's function associated with the Bloch wave function. It requires the expression of the Green's function in the Fourier domain.[13] The slowness s_x is now connected to the propagation parameter γ via the relation $s_x = 2\pi\gamma/(\omega p) = \gamma/(fp)$. As in the nonperiodic case, Eq. (10) is inserted in the left hand side of Eq. (1), yielding the following relations:

$$\int\int_{\Gamma} \delta u_i T_{ij} n_j dS = -\sum_{e,\varepsilon=1}^{E}\sum_{l=-\infty}^{+\infty} \frac{1}{p}\tilde{G}(\gamma + l, \omega) \times \int_{\Gamma e} \sum_{n=1}^{Nd(e)} P_n(x)e^{-j\frac{2\pi}{p}(\gamma+l)x}dx \times \delta u^{*(n,e)}_{\text{normal}} \times \int_{\Gamma\varepsilon} \sum_{m=1}^{Nd(\varepsilon)} P_m(x')e^{j\frac{2\pi}{p}(\gamma+l)x'}dx' u^{(m,\varepsilon)}_{\text{normal}}. \tag{11}$$

In Eq. (11) , $P_n(x)$ is the nth interpolation polynomial of the current element e (E is the total number of radiating elements) exhibiting Nd nodes. It can be remarked that the integrals in Eq. (11) do not depend on the frequency. This property is used to optimize the computation time. Also the two integrals are complex conjugated, providing again a possibility to optimize the computation code. However, it can be also pointed out that no other particular symmetry can be found in this expression. The radiation matrix of the periodic problem written $X^{(P)}$ is then a general complex matrix and must be computed for all values of γ and ω. The problem to be solved is finally written as

$${}^t[T_u^*(\gamma)][K_{uu} - \omega^2 M_{uu} - X^{(p)}(\gamma, \omega)][T_u(\gamma)]\{v\} = {}^t[T_u^*(\gamma)]\{F\}. \tag{12}$$

As in the case of Eq. (6), the mass and stiffness matrices K_{uu} and M_{uu} are symmetric and complex (M_{uu} is real positive but K_{uu} takes acoustic losses into account). The final matrix of the algebraic problem to be solved is then complex nonsymmetric. Since a lot of its components are equal to zero, one can advantageously use a sparse matrix solver dedicated to that kind of problem.[16]

Figures 4 and 5 show how the nonperiodic and periodic approaches can be used to analyze a cMUT radiating in water. Figure 4 shows a comparison between the normal mechanical displacements computed for only one cell of a cMUT array using the nonperiodic approach and the same result using the periodic Green's function calculation. In both cases, the resonance is dramatically shifted down to low frequencies. However, in the case of nonperiodic computations, the normal displacements still exhibit a true resonance contribution with a well-marked phase variation whereas the periodic calculation results indicate a slowly varying magnitude of the displacement with no phase rotation. A convergence test has been then performed to check the relation between periodic and nonperiodic computation. The

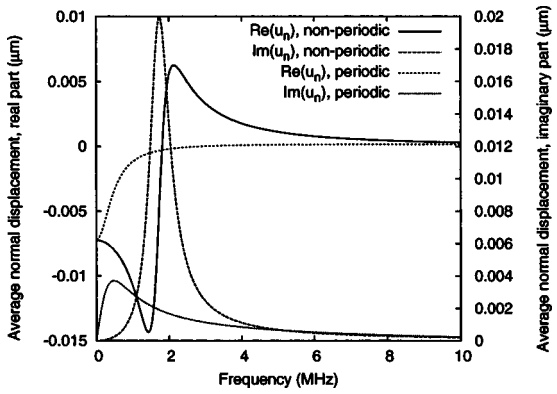

FIG. 4. Comparison between periodic and nonperiodic computation of a cMUT elementary cell radiating in water.

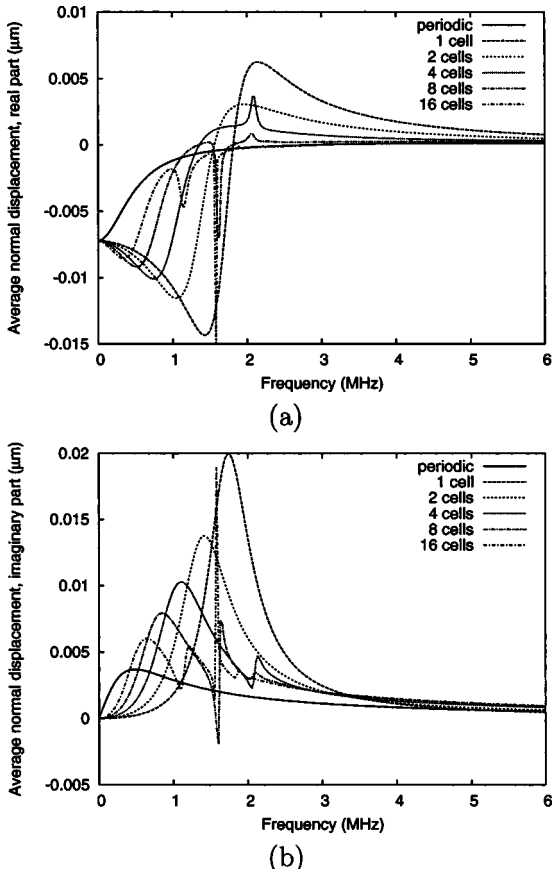

FIG. 5. Convergence of the nonperiodic computations toward the periodic result. (a) Real part of u_n. (b) Imaginary part of u_n.

Downloaded 21 Jan 2005 to 195.83.19.253. Redistribution subject to AIP license or copyright, see http://jap.aip.org/jap/copyright.jsp

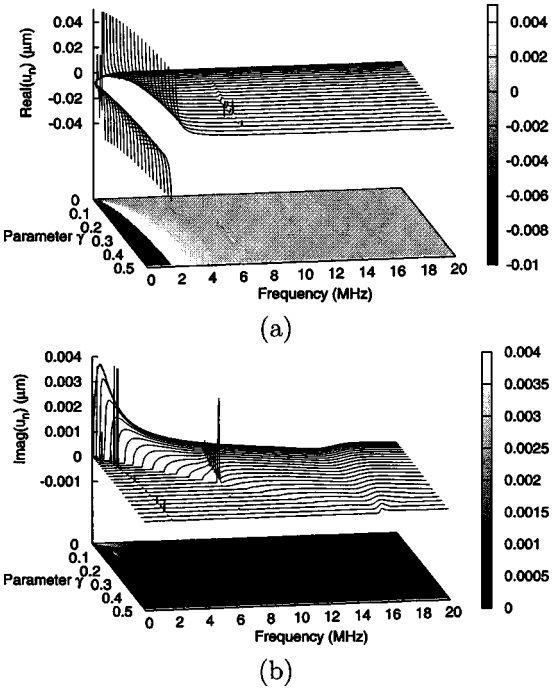

FIG. 6. Normal displacement u_n of a periodic cMUT array loaded by water vs excitation parameter γ and angular frequency ω. (a) Real part of u_n. (b) Imaginary part of u_n.

number of cells has been extended to 2, 4, 8, and 16 in the nonperiodic calculations and the results are compared again to the periodic case (see Fig. 5).

One can easily see that the convergence of the nonperiodic case toward the periodic one rapidly arises. The frequency is shifted down together with the number of cells, as well as the magnitude of displacement. The origin of the parasitic contributions on the 4, 8, and 16 cell computations is not identified yet.

Dispersion effects have been also computed by simply varying the propagation parameter γ from 0 to 0.5. Plotting the corresponding displacements versus γ and ω allows one for identifying the acoustic phenomena related to the periodic nature of the transducer, and particularly the crosstalk effects due for instance to modes guided along the structure. Figure 6 shows the mean normal displacement versus γ and ω in the expected operation domain.

It appears that for a propagation parameter different from zero (not all the cells vibrating in phase), at least two modes can be guided by the structure, one at rather low frequencies (up to 2 MHz) and another one exhibiting a smaller contribution to the normal displacement at 6 MHz. The first one may correspond to a wave guided at the interface cMUT/water, exhibiting a behavior similar to that of a Stoneley wave.[13] The second one may correspond to a second harmonic of the 2 MHz guided wave. To better understand the influence of these contributions to the actual operation of the cMUT array, the derivation of mutual displacement from the harmonic calculation has been investigated. We lay down that the constant homogeneous active force F is related to the mean normal displacement $\overline{u_n}$ of the membrane via a scalar value H as follows:

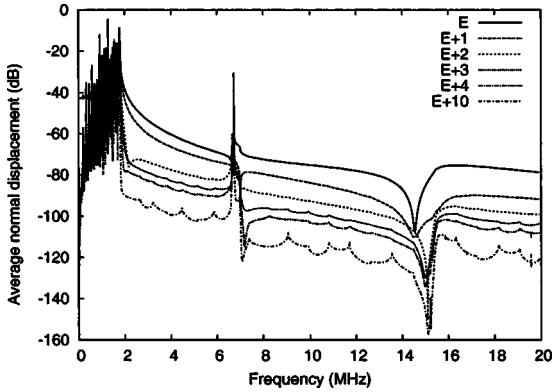

FIG. 7. Mutual normal displacements $|u_n|$ of a periodic cMUT array loaded by water. E denotes the central excited cell, $E+n$ the nth neighbour of cell E.

$$\overline{u_n}(\gamma,\omega) = H(\gamma,\omega)F. \tag{13}$$

For a unit value of excitation force, $\overline{u_n}$ is equivalent to H which is called here "harmonic mechanical coupling." It is then possible to deduce the mutual mechanical coupling from the harmonic mechanical coupling by Fourier transform, similarly to the calculation of mutual electrical admittance from harmonic admittance[7]

$$H_m(\omega) = \int_0^1 H(\gamma,\omega)e^{j2\pi m\gamma}d\gamma. \tag{14}$$

For a unit force excitation, the mutual mechanical coupling is equivalent to the mean normal displacement generated by the earlier mentioned force on the neighboring cells of the excited one. The integration of Eq. (14) is performed using a numerical integration scheme requiring at least 30 Gauss points along γ (for each frequency) to correctly take into account the sharp variations of the harmonic displacement due to wave guided at the interface between the membrane and the radiation domain. Figure 7 shows the computation results for the ten closer neighbors of the excited cell. The mutual displacement curves exhibit sharp variations from 0 to 2 MHz typically due to the guided mode identified in Fig. 6. This indicates a very large amount of crosstalk in that frequency range. Also the mode at 6 MHz provides a visible contribution even if 10–20 dB smaller than the ones at 2 MHz. In both cases, the modes propagate along the array with almost no loss, according to their narrow contributions to the imaginary part of the harmonic normal displacement. It is also shown that if the mutual displacements could be cleared of these contributions, the amount of crosstalk would decrease rapidly along the array (rejection better than 20 dB for the third neighbor, better than 40 for the tenth neighbor).

III. SIMPLIFIED ANALYSIS OF THE ELECTRIC RESPONSE OF A CMUT

Since the basic principle of cMUTs consists in generating electrostatic forces between the two electrodes of a planar capacitor, the simulation of the electrical response of such devices requires the computation of a capacitance taking into account the vibration modulating the gap between the two earlier mentioned electrodes.[17] Although an accurate

Downloaded 21 Jan 2005 to 195.83.19.253. Redistribution subject to AIP license or copyright, see http://jap.aip.org/jap/copyright.jsp

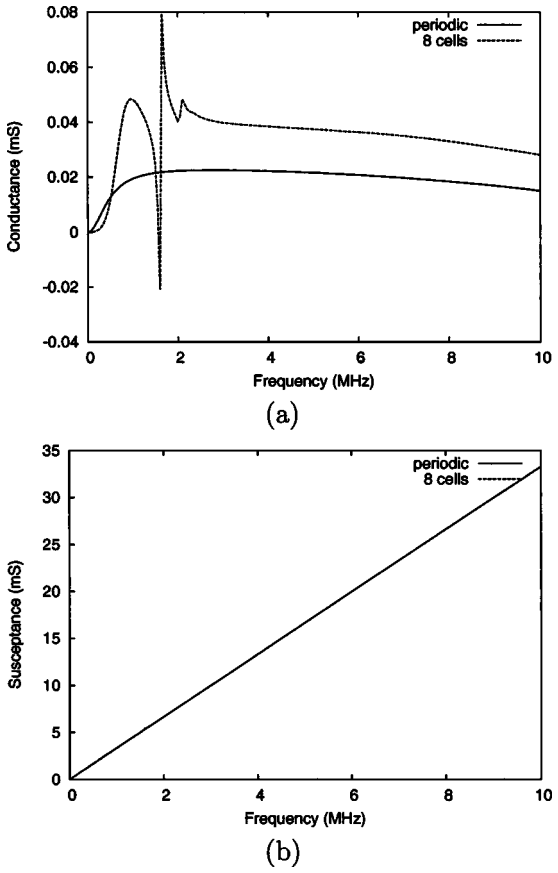

FIG. 8. Comparison between cMUT admittances of an eight-cell array and of a periodic device computed with the proposed simplified model based on planar capacitance formulae.

estimation of the generated force would require the exact computation of the charge distribution on the electrodes due to the application of a potential difference as well as the estimation of the actual gap when applying the dc bias voltage, a simplified approach can be considered first. One can easily calculate the force generated in a planar capacitor by using the classical capacitance formula. It is inserted in the electrostatic energy relation which is then differentiated versus the capacitor gap (y) to access the normal force applied on the deformable electrode. This yields the following form of this force:

$$F_y = -\frac{\partial U}{\partial y} = -\frac{1}{2}\frac{\partial (CV^2)}{\partial y} = \frac{\varepsilon S V^2}{2y^2}. \tag{15}$$

This relation does not take into account the effects due to charge concentration at the edge of the electrodes but is known as a good estimation of the generated force resulting in a correct estimation of the electromechanical phenomena arising in air or vacuum-gap capacitors. However, one can simply compute the capacitance variations due to the dynamic vibration using the standard planar capacitor formula. Let us consider now that the value of the gap is given by $g = y + u_n(\omega)$, i.e., the static value of the gap plus the normal dynamic displacement. The definition of an admittance (for a 1 V excitation) is given by

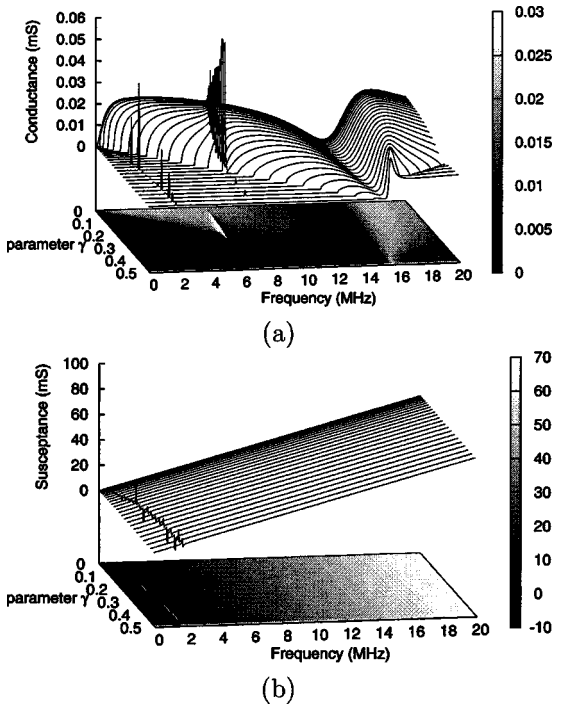

FIG. 9. Harmonic admittance Y of a periodic cMUT array loaded by water (proposed simplified model). (a) Real part of Y. (b) Imaginary part of Y.

$$Y = \frac{j\omega Q}{V} = j\omega \frac{\varepsilon S}{g}, \tag{16}$$

where Q is the electrical charge. Considering a complex value of this normal displacement yields the following expression of Y

$$Y = \frac{\mathrm{Im}(u_n)\omega\varepsilon S}{[y - \mathrm{Re}(u_n)]^2 + \mathrm{Im}(u_n)^2} + j\frac{[v - \mathrm{Re}(u_n)]\omega\varepsilon S}{[y - \mathrm{Re}(u_n)]^2 + \mathrm{Im}(u_n)^2}, \tag{17}$$

where $\mathrm{Re}(u_n)$ and $\mathrm{Im}(u_n)$, respectively, holds for the real and imaginary parts of the normal displacements. One can simply apply this formula using the results of periodic as well as nonperiodic computations to have a rough idea of the admittance of cMUTs. Figure 8 shows a comparison between the admittances of a reduced cMUT array (eight cells) and of a periodic array.

This comparison shows that the periodic device exhibits an almost flat conductance in the frequency bandwidth 1–6 MHz and a capacitive susceptance very comparable to the one of the eight-cell cMUT array. The later exhibits a conductance with sharp contributions in the vicinity of 2 MHz, corresponding to the rapid variations of the normal displacement observed in Fig. 5. If this result is confirmed experimentally, this means that below a critical number of cells, the transducer bandwidth may be reduced due to undesirable low frequency vibrations. It is also possible to compute the mutual admittance in that way. The harmonic admittance is plotted in Fig. 9 and the corresponding mutual terms are reported in Fig. 10, yielding the same observations as for harmonic and mutual displacements.

Downloaded 21 Jan 2005 to 195.83.19.253. Redistribution subject to AIP license or copyright, see http://jap.aip.org/jap/copyright.jsp

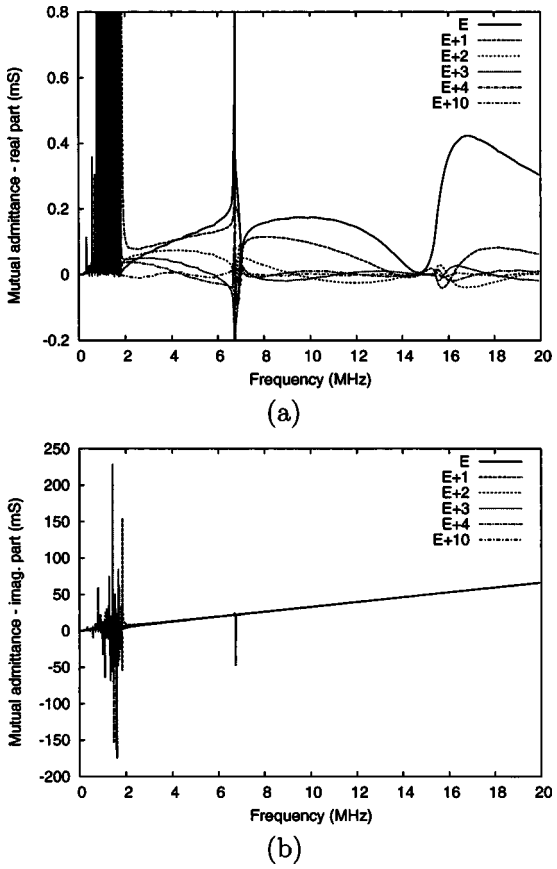

FIG. 10. Mutual admittances Y_n of a periodic cMUT array loaded by water (proposed simplified model). E denotes the central excited cell, $E+n$ the nth neighbor of cell E. (a) Real part of Y_n. (b) Imaginary part of Y_n.

IV. CONCLUSION

The development of an accurate simulation tool allowing one to take periodicity of cMUTs into account provides an extended analysis of the operating principles of such devices under different conditions. The comparison with nonperiodic computations shows that both approaches tend to provide similar results, but with a dramatic gain in computation time when using the periodic analysis instead of meshing a large number of elementary cells in the nonperiodic approach to simulate periodic devices. Moreover, the periodic analysis offers better and direct understanding of what may happen if synchronous defects arise in the array, or more generally if phase shifts are generated in a given combination of cMUT arrays. The capability of such devices to guide acoustic waves at the interface with water may generate large crosstalk effects, for instance able to degrade the operation of a cMUT-based imaging probe. Of course, these theoretical results have to be confirmed by experiments. Nevertheless, it must be emphasized that a good agreement has been obtained comparing periodic and nonperiodic computations with radiation boundary conditions (both numerical codes are perfectly independent and significantly different in substance). The nonperiodic computation was already found reliable when compared with experiments. Finally, the analysis of cMUT excited with particular phase sequence shows that cMUT-based devices are particularly able to generate interfacial propagation phenomena, with an evanescent wave in the fluid.

ACKNOWLEDGMENTS

This work was partly supported by the EUREKA Bureau as the UMIC project. The authors want to thank W. Steichen, R. Lardat, and Th. Pastureaud from Temex, and J. F. Gelly and F. Lantéri from General Electric Parallel Design SAS, for fruitful discussions.

[1] B. T. Khuri-Yakub, F. L. Degertekin, X. C. Jin, S. Calmes, I. Ladabaum, S. Hansen, and X. J. Zhang, Proc. of the IEEE Ultrasonics Symposium, 1998, pp. 985–991.
[2] A. Caronti, G. Caliano, A. Iula, and M. Pappalardo, IEEE Trans. Ultrason. Ferroelectr. Freq. Control **2**, 159 (2002).
[3] M. I. Haller and B. T. Khuri-Yakub, Proc. of the IEEE Ultrasonics Symposium, 1994, pp. 1241–1244.
[4] A. Rønnekleiv, P. E. Roche, and B. T. Khuri-Yakub, Proc. of the IEEE Ultrasonics Symposium, 1997, pp. 1061–1065.
[5] G. G. Yarogliu, A. S. Ergun, B. Bayram, E. Haeggström, and B. T. Khuri-Yakub, Proc. of the 2nd international workshop on MUTs, Besançon, France, 2002, pp. 37–41.
[6] M. Kaltenbacher, H. Landes, K. Niederer, and R. Lerch, Proc. of the IEEE Ultrasonics Symposium, 1999, pp. 1155–1158.
[7] S. Ballandras, M. Wilm, P.-F. Edoa, A. Soufyane, V. Laude, W. Steichen, and R. Lardat, J. Appl. Phys. **93**, 702 (2003).
[8] G. Schröpfer, S. Ballandras, M. de Labachelerie, P. Blind, and Y. Ansel, J. Micromech. Microeng. **7**, 71 (1997).
[9] G. S. Kino, *Acoustic Waves, Devices, Imaging and Analog Signal Processing* (Prentice-Hall, Englewood Cliffs, NJ, 1987).
[10] Modulef official website, url http://www-rocq.inria.fr/modulef/english.html.
[11] A. Caronti, H. Majjad, S. Ballandras, G. Caliano, R. Carotenuto, A. Iula, V. Foglietti, and M. Pappalardo, IEEE Trans. Ultrason. Ferroelectr. Freq. Control **49**, 289 (2002).
[12] Y. Roh and B. T. Khuri-Yakub, IEEE Trans. Ultrason. Ferroelectr. Freq. Control **49**, 293 (2002).
[13] J. D. Achenbach, *Waves Propagation in Elastic Solids* (Elsevier Science, North Holland, 1975).
[14] D. Royer and E. Dieulesaint, *Elastic Waves in Solids 1* (Springer, Berlin, 2000).
[15] V. P. Plessky and Th. Thorvaldsson, IEEE Trans. Ultrason. Ferroelectr. Freq. Control **42**, 280 (1995).
[16] T. A. Davis and I. S. Duff, SIAM J. Matrix Anal. Appl. **18**, 140 (1997).
[17] D. Griffiths, *Introduction to Electrodynamics* (Prentice-Hall, Englewood Cliffs, NJ, 1981), pp. 291–292.

Downloaded 21 Jan 2005 to 195.83.19.253. Redistribution subject to AIP license or copyright, see http://jap.aip.org/jap/copyright.jsp